Bulletin of Engineering Geology and the Environment (2022) 81: 117
https://doi.org/10.1007/s10064-022-02621-2

ORIGINAL PAPER

Strength variations due to re-liquefaction—indication from cyclic tests on undisturbed and remold samples of a liquefaction-recurring site

Fu-Kuo Huang[1] · Chi-Chin Tsai[2] · Louis Ge[3] · Chih-Wei Lu[4] · Chung-Chi Chi[5]

Received: 5 July 2021 / Accepted: 17 February 2022 / Published online: 23 February 2022

Abstract
According to historical records, the soil in the Xinhua District of Tainan City, Taiwan, has been liquefied several times in 1946, 2010, and 2016. To assess the soil liquefaction resistance and understand the recurring liquefaction mechanism of this site, this study conducts a series of experimental tests, including the undrained dynamic triaxial tests on undisturbed and remolded soil samples retrieved from the site. Different fines contents, dry densities, and effective confining pressures are considered for the remolded samples during the test program to investigate their influence on the soil liquefaction resistance. A complete experimental soil liquefaction resistance curve of the site is constructed based on the test results. The liquefaction resistances of the undisturbed and remolded samples were found to be similar at the recurring liquefaction site in the present study. Besides, the experimental soil liquefaction resistance curve of the recurring liquefaction site was lower than the in situ empirical soil liquefaction resistance curve that is based on all site conditions, including the aging effect. This observation agrees with the other laboratory test and field investigation that the triggered liquefaction leads to the "reset" of the aging effect that lowers the liquefaction resistance. The finding of this study may explain why a recurring liquefaction site is more vulnerable to liquefaction in a seismic event.

Keywords Cyclic triaxial test · Undisturbed sample · Remolded sample · Soil liquefaction resistance curve · Aging effect

Introduction

Based on observations from past earthquakes, soil liquefaction typically occurs in artificial lands or young alluvium deposits, whereas it is not observed in old alluvium deposits at the same ground shaking intensity. During the 1999 Chi-Chi earthquake in Taiwan (Mw = 7.6), severe liquefaction damages were reported at Taichung harbor that was made using artificial fills (Huang and Yang 2001). During the 2011 Tohoku earthquake in Japan (Mw = 9.0), liquefaction occurred extensively along the Tokyo bay area, particularly in Urayasu city, which was newly reclaimed after 1968 by the hydraulically filling of sea-bed soils (Kokusho 2016; Towhata et al. 2017). In contrast, another area of the same city that existed before 1948 did not liquefy, despite very similar soil profiles and soil properties (Kokusho 2016). During the 2016 Meinong earthquake (Mw = 6.4) in Taiwan, only localized liquefaction was reported in reclaimed areas that were used to be fish ponds in the early 1960s, whereas the other places near the epicenter were free from liquefaction damage (Tsai et al. 2017).

Youd and Hoose (1977) and Youd and Perkins (1978) noted that liquefaction resistance increases markedly with geologic age. Sediments deposited within the last few thousand years are generally much more susceptible to liquefaction than older Holocene sediments. Pleistocene sediments are even more resistant, and pre-Pleistocene

✉ Chi-Chin Tsai
tsaicc@nchu.edu.tw

1 Department of Water Resources and Environmental Engineering, Tamkang University, Taipei, Taiwan

2 Department of Civil Engineering, National Chung Hsing University, Taichung, Taiwan

3 Department of Civil Engineering, National Taiwan University, Taipei, Taiwan

4 Department of Civil and Construction Engineering, National Taiwan University of Science Technology, Taipei, Taiwan

5 Environmental Engineering Geology Division, Central Geology Survey, Taipei, Taiwan

sediments are generally immune to liquefaction. In contrast, after conducting laboratory tests, several investigators have noted that the liquefaction resistance of soils increases with age (Arango and Migues 1996; Bwambale et al. 2017; Chen and You 2004; Hayati and Andrus 2009; Ishihara 1985; Kiyota et al. 2009; Kokusho et al. 2012; Ladd 1982; Moss et al. 2008; Seed 1979; Tatsuoka et al. 1988; Taylor 2015; Troncoso et al. 1988). Seed (1979) observed significant increases in liquefaction resistance with aging of remolded sand specimens tested in the laboratory. Increases of as high as 25% in the cyclic resistance ratio between the freshly remolded and 100-day-old specimens were noted.

Past studies on causative mechanisms of aging can be classified into two groups. The first group advocates cementation (Kokusho et al. 2012). For instance, Mitchell and Solymer (1984) considered the sedimentation of silicate material at granular contacts as a bonding mechanism. The second group concerns the change in granular packing induced by weak ground vibrations (Dobry et al. 2015; Kiyota et al. 2009; Kondo 2013; Wichtmann et al. 2005). Studies on this concept have noted that the induced dislocation of sand grains causes large voids to be filled; improves the mechanical stability of soil structures, intergranular locking, or the number of grain contacts; and increases the liquefaction resistance. Field observations and centrifuge modeling suggest that pre-shaken natural sands located in the Imperial Valley of California, USA, have high liquefaction resistance as a result of pre-shaking (El-Sekelly et al. 2016a, b).

In contrast to the benefit of the aging effect that increases liquefaction resistance, a site that has already been liquefied has a high potential for liquefaction in the future (Quigley et al. 2013; Tsai et al. 2017; Wakamatsu 2012; Youd 1984). For example, following the 2010 Mw 7.1 Darfield earthquake, ten distinct liquefaction episodes were recorded in eastern Christchurch, New Zealand, within a year. Sand blow activity was caused by a sequence of earthquakes (Mw 5.2–7.1) with a peak ground acceleration (PGA) as low as 0.057 g, which typically cannot trigger liquefaction (Quigley et al. 2013). The reason for high liquefaction vulnerability at a site that has been subjected to recurring liquefaction could be also associated with the aging effect. Many laboratory studies have indicated that the aging effect is "reset" once liquefaction occurs (Dobry and Abdoun 2015; El-Sekelly et al. 2016a, b; Goto and Towhata 2014; Okamura et al. 2019). In other words, the aging effect is eliminated due to the large strain induced during liquefaction and, thus, the re-liquefaction resistance is low as observed in the recent multiple liquefaction tests (Amini et al. 2021; Darby et al. 2019; Price et al. 2017; Teparaksa and Koseki 2018; Wahyudi et al. 2016; Ye et al. 2018).

To assess the soil liquefaction resistance of a site subjected to recurring liquefaction and the associated aging effect, this study uses boring samples from a farmland site in the Xinhua District of Tainan City (Fig. 1), where liquefaction occurred repeatedly during the 1946 Xinhua earthquake, the 2010 Taoyuan earthquake, and the 2016 Meinong earthquake (Tsai et al. 2017). A field reconnaissance was conducted by Tsai et al. (2017) immediately after the 2016 Meinong earthquake, where the observed geotechnical damage features, including soil liquefaction, were summarized. Tsai et al. (2020) further assessed soil liquefaction, building settlement, and residual strength in two residential areas during the Meinong earthquake via field investigation and thorough numerical analysis. Yet no detailed investigation has been performed on the recurring liquefaction site. Therefore, in the present study, a series of saturated undrained cyclic triaxial tests were conducted on the undisturbed and remolded soil samples to construct a complete soil liquefaction resistance curve for the site based on the test results. Furthermore, test results of the undisturbed and remolded samples were compared to understand the effect of aging on soil liquefaction resistance. Remolded samples were prepared under the same conditions as the in situ conditions. Different fine contents (FCs), dry densities, and effective confining pressures were considered to investigate their effects on soil liquefaction resistance. Subsequently, an experimental soil resistance curve was constructed and compared to the in situ empirical soil liquefaction resistance curve to discuss the aging and recurring liquefaction effect.

Background of liquefaction reoccurrence site

Historically, Xinhua has been subjected to several soil liquefaction phenomena induced by earthquakes such as the 1946 Xinhua earthquake, the 2010 Taoyuan earthquake, and the 2016 Meinong earthquake. The magnitude of these earthquakes, focal depth, PGA at the Xinhua liquefaction site, and the liquefaction area are listed in Table 1. In 2016, the Meinong earthquake caused wide-area sand boils in farmland and irrigation channels of the Beishi and Taiping villages (Fig. 1). Although soil liquefaction did not lead to severe damage, the liquefaction area (as observed by the sand boils) was widely distributed from the Taiwan high-speed railway (THSR), Puxian temple, to the Xinhua bypass (Fig. 1). Compared to the 2010 Taoyuan earthquake, the area of the sand boil created during the 2016 Meinong earthquake was found to be greater. As indicated in Fig. 1, the liquefaction sites observed after these three earthquakes considerably overlapped with each other. Figure 2 shows the sand boils observed at the same location during the 2010 Taoyuan and the 2016 Meinong earthquakes.

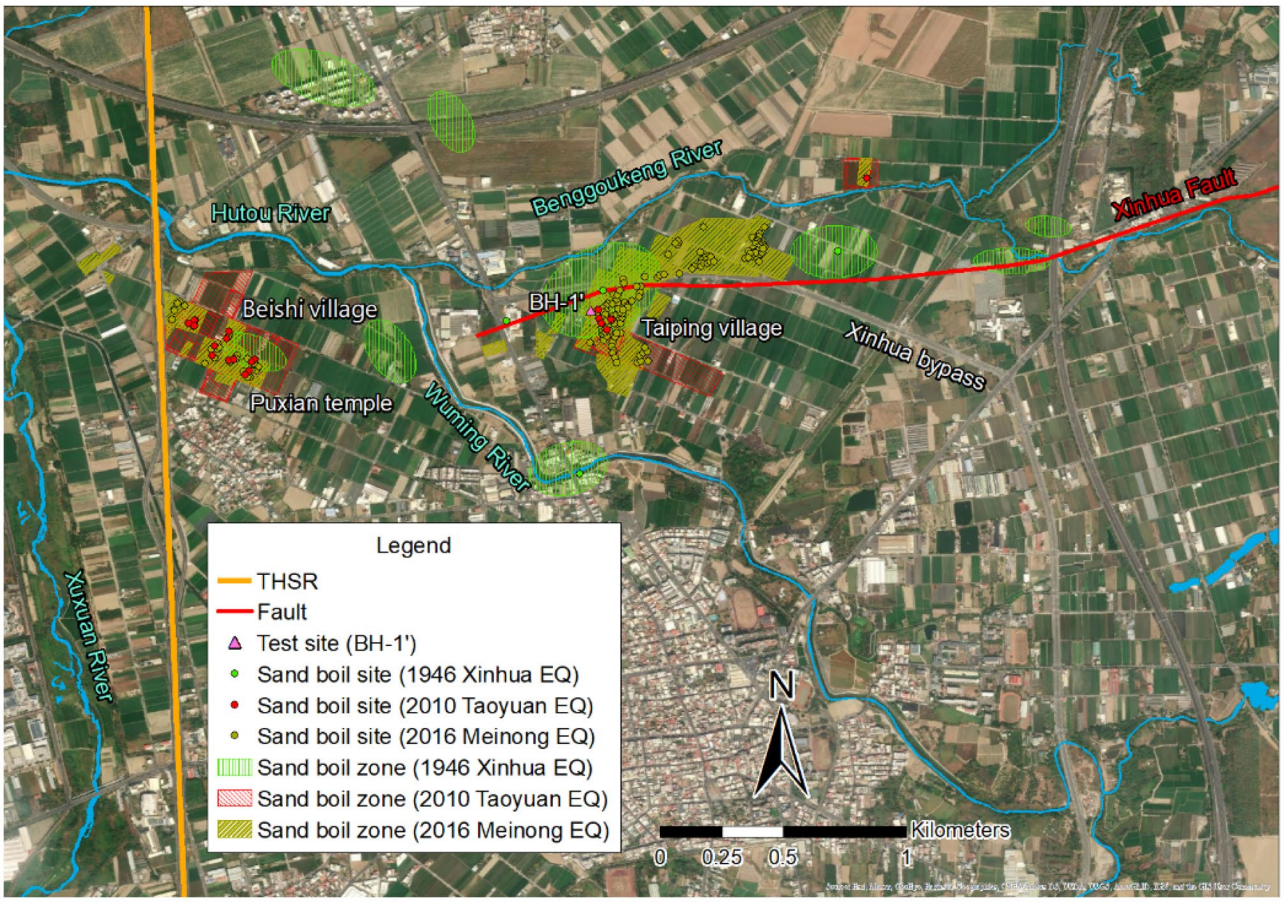

Fig. 1 Sand boil locations during the 1946 Xinhua earthquake, the 2010 Taoyuan earthquake, and the 2016 Meinong earthquake

The liquefaction area observed during the 2010 Taoyuan earthquake was the largest in the Beishi village (located to the west of the research site) of the Xinhua District, Tainan, whereas the liquefaction area observed during the 2016 Meinong earthquake was closer to the THSR, and its impact on the THSR is worthy of investigation. The sand boils caused by the 2016 Meinong earthquake were also widely spread in the Taiping village (located across the Xinhua Fault). Although the area of sand boils caused by the 1946 Xinhua earthquake was not large, many liquefaction sites were distributed over a wide area.

The re-liquefaction area is located in the transition zone between the coastal plain and foothills. The coastal plain region is primarily Holocene sedimentary deposits consisting of silt, clay, and sand. Relatively fine sediments are transported from the Central Range of Taiwan following the weathering of shale, slate, and mudstone. These soil sediments are typical sedimentary materials of the southwestern plain of Taiwan. The Xinhua fault, the main source of seismicity in the 1946 Xinhua earthquake, is an oblique fault with right lateral and reverse movement. The fault is classified as a Type I active fault according to the Central Geological Survey. The fault

Table 1 Information of three earthquakes that caused soil liquefaction at the Xinhua site

No	Earthquake	Date	Magnitude (M_L)	Focal depth (km)	PGA (g)	Liquefaction area (km^2)
1	Hsinhua	December 5, 1946	6.1	5.0	Level V*	0.42
2	Taoyuan	March 4, 2010	6.4	22.6	0.13–0.15	0.23
3	Meinong	February 6, 2016	6.6	14.6	0.25–0.30	0.36

*PGA = 80 ~ 250 gal

(a) 2010 Taoyuan earthquake **(b)** 2016 Meinong earthquake

Fig. 2 Sand boil near Puxian temple during the 2010 Taoyuan earthquake and the 2016 Meinong earthquake. **a** 2010 Taoyuan earthquake. **b** 2016 Meinong earthquake

line, with strike direction of N70°E, extends from the Naba village to the west of the Beishi Village with a total length of 6 km. In addition to high seismicity, this reliquefaction area also has many rivers passing nearby, as indicated in Fig. 1. In addition, the groundwater level is shallow. Therefore, the liquefaction potential of this area is high.

A boring of 30 m (BH-1') was drilled to investigate the subsurface condition of the study site (Fig. 1). As shown in Fig. 3, the site is composed of an interlayer of silty sand (SM), silt (ML), and clay (CL). The ground water table is 0.13 m below the ground surface. The shallow SM/ML layers within a depth of 8 m exhibit a high liquefaction potential, given that the *N*-values of the standard penetration test (SPT) are mostly below 10 and shear wave velocities (Vs) are less than 200 m/s.

Six undisturbed soil samples were retrieved using the well-documented Gel-push sampling method (Lee et al. 2012; Taylor et al. 2012; Umehara et al. 2015). The Gel-push sampling method uses non-circulated polymer solution of high concentration as its drilling fluid for lubricant. The polymer solution is coated on a surface of a soil sample, and reduces friction between the sample tube and the sample during the sampling process. These Gel-push samples (1-m long), being intended to cover ML, SM, and CL, were obtained at the adjacent borings (BT-1 and BT-1', 3.78 m and 3.04 m away from BH-1', respectively). The depths of these samples and associated sample numbers are indicated in Fig. 3.

Laboratory test program

Undisturbed sample

Cyclic triaxial tests were performed on undisturbed samples to determine the soil liquefaction resistance. For each 1-m undisturbed samples, four cyclic triaxial tests (7 cm in diameter and 15 cm in height) were performed. The cyclic stress ratio (CSR) was defined as follows:

$$\mathrm{CSR} = \frac{q}{2\sigma_c'} \tag{1}$$

where q is the cyclic deviatoric stress and σ_c' is the effective confining pressure. Therefore, a total of 12 tests were conducted for different types of soil. Before applying the cyclic shearing load, the soil samples were isotopically consolidated to the in situ mean stress, as indicated in Table 2. Next, cyclic deviatoric stress was applied at a frequency of 1 Hz under undrained conditions. Ishihara (1993) suggested that excess pore water pressure ratio (r_u) reaches 0.9–0.95 as the state of liquefaction failure for overcoming the problem where researchers often report the difficulty of achieving unity r_u in laboratory tests, especially for the soil with high FCs. Once r_u of 0.9 ~ 0.95 is built up, a sizeable amount of cyclic strain is observed to develop, indicating considerable softening or failure taking place in these soils. Therefore, the test was stopped when the r_u reached 0.95, which was defined as the state of failure, and the corresponding number of cycles was defined as N_f. Subsequently, soil property tests (e.g., gradation and plasticity) were conducted on the tested soil samples.

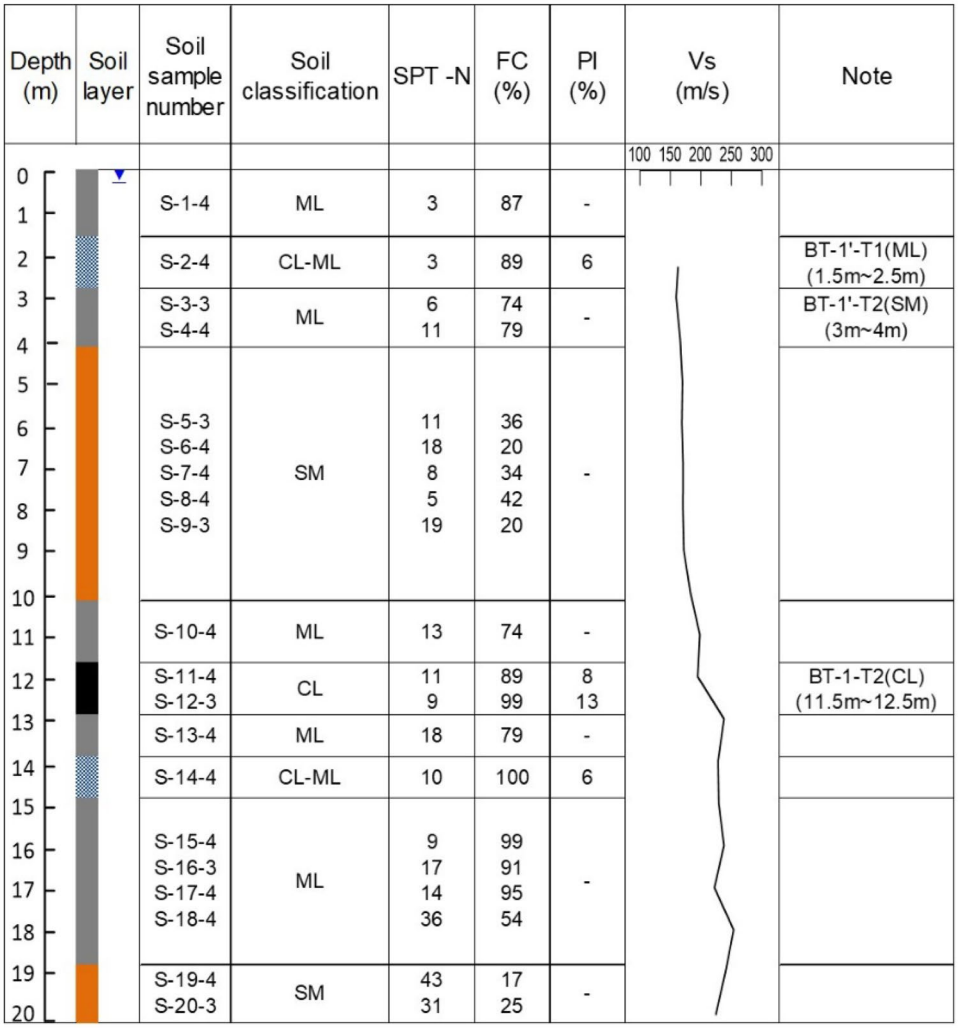

Fig. 3 Boring log and Vs of BH-1'

Remolded sample

The soil liquefaction resistance can be determined by testing a remolded sample under a wide range of conditions. Table 3 lists all reconstitutive conditions considered in the test program. A remolded sample (Set 1) is prepared to reproduce the field conditions of the BT-1'-T2 sample that represents the liquefied layer. To prepare the remolded samples, the tested undisturbed samples were oven-dried, sieved, re-mixed, and compacted into molds to achieve the same

Table 2 Tests performed on undisturbed samples for liquefaction resistance

Boring no	Depth (m)	Sample no	Soil type	Confining pressure (kPa)	CSR	N_f
BT-1'	1.5–2.5	T1-1	ML	14	0.309	13
		T1-2	SM	14	0.205	219
		T1-3	ML	14	0.245	31
		T1-4	SM	14	0.352	4
BT-1'	3.0–4.0	T2-1	ML	24	0.158	1411
		T2-2	SM	24	0.34	7
		T2-3	ML	24	0.305	40
		T2-4	ML	24	0.242	746
BT-1	11.5–12.5	T2-1	CL	76	0.307	25
		T2-2	SC	76	0.341	78
		T2-3	SC	76	0.357	48
		T2-4	SC	76	0.504	4

Table 3 Tests performed on remolded samples

Test set	FC (%)	Confining pressure (kPa)	γ_d(t/m^3)	CSR	N_f
1	50	24	1.66	0.14	5287
			1.67	0.3	28
			1.66	0.34	32
			1.7	0.36	14
			1.67	0.25	74
			1.7	0.2	511
			1.67	0.37	10
2	50	100	1.68	0.3	4
		50	1.67	0.3	6
		30	1.67	0.3	6
3	35	24	1.68	0.2	130
			1.69	0.25	26
			1.67	0.3	13
4	12	24	1.67	0.2	65
			1.69	0.25	19
			1.67	0.3	6
5	5	24	1.67	0.2	34
			1.67	0.25	11
			1.69	0.3	5
6	5	24	1.55	0.15	6
			1.41	0.12	7
			1.52	0.12	18
			1.61	0.18	18
			1.73	0.23	832

dry unit weight (γ_d) and FC as that in the field. Different remolded samples were prepared for various values of γ_d (Set 6) and FC (Set 3–5). Moreover, different consolidation pressures (Set 2) were considered during the consolidation stage of the test. Similar to the test procedure of the undisturbed sample, the soil samples were isotopically consolidated to the target pressure (Table 3). It should be noted that the remolded γ_d after the compaction and that after the consolidation is similar, especially for Set 1; thus, the remolded specimen can represent the field condition. After the consolidation stage, cyclic deviatoric stress was applied at a frequency of 1 Hz. The test was stopped when r_u reached 0.95, and the value of N_f was determined accordingly.

Test results

Physical properties

Figure 4 shows the grain size distribution curve of the undisturbed samples, including BT-1'-T1, BT-1'-T2, and BT-1-T2. For the BT-1'-T2 sample, all grain size distributions are similar except for T2-4, which is located at the bottom of the 1-m long tube. The grain size distribution is non-uniform with a uniformity coefficient (Cu) of 1.2. The FC is approximately 50% and the fines are non-plastic (NP). The BT-1'-T1 and BT-1-T2 samples exhibit a similar grain size distribution that is better graded compared to the BT-1'-T2 sample. However, the FCs of the BT-1'-T1 and BT-1-T2 samples are mostly less than 50% (ranging from 25 to 60%), indicating that these samples are more like SM or SC rather than CL-ML or CL as characterized in Boring BH-1' according to the Unified Soil Classification System. The plasticity indices (PIs) of the BT-1'-T1 and BT-1-T2 samples are 0–10% and 10–19%, respectively; however, the BT-1'-T1 sample had a higher FC (38 ~ 60%) than the BT-1-T2 sample (35 ~ 52%). Overall, these samples are susceptible to soil liquefaction in terms of FC and plasticity, which will be discussed later in more detail.

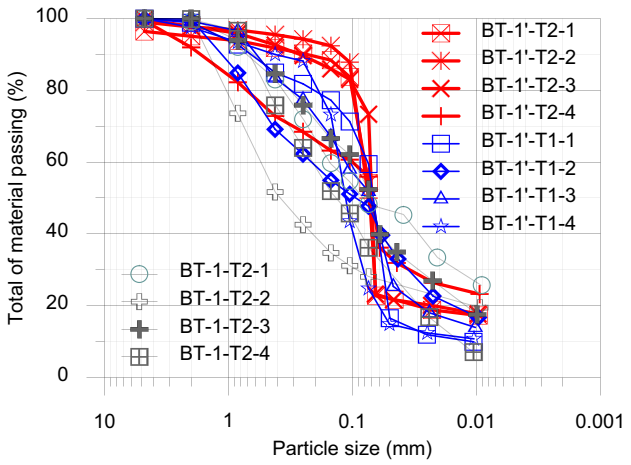

Fig. 4 Grain size distribution curve of the undisturbed sample. Red, blue, and black curves indicate the BT-1'-T2, BT-1'-T1, and BT-1-T2 samples, respectively

Liquefaction resistance from undisturbed sample

Figure 5 shows an example of the stress-controlled cyclic triaxial test result (BT-1-T2-3) to obtain liquefaction resistance. During this test, the applied cyclic stress remains the same with cycles (Fig. 5a), whereas the resulting cyclic strain increases with cycles (Fig. 5b). As the number of cycles increases, the pore water pressure accumulates (Fig. 5c). Meanwhile, the stress–strain loop tilts (i.e., shear modulus degrades, Fig. 5d), and thus, the strain increases. Finally, the sample reaches its initial liquefaction point (i.e., $r_u = 0.95$) at the 40th cycle (i.e., $N_f = 40$). Similar observations were made in the other tested specimens.

Figure 6 shows the comparison of the liquefaction resistances obtained from the cyclic test results of BT-1'-T1, BT-1'-T2, and BT-1-T2. BT-1-T2 (PI = 10 ~ 19%) exhibits a higher liquefaction resistance than the others, as

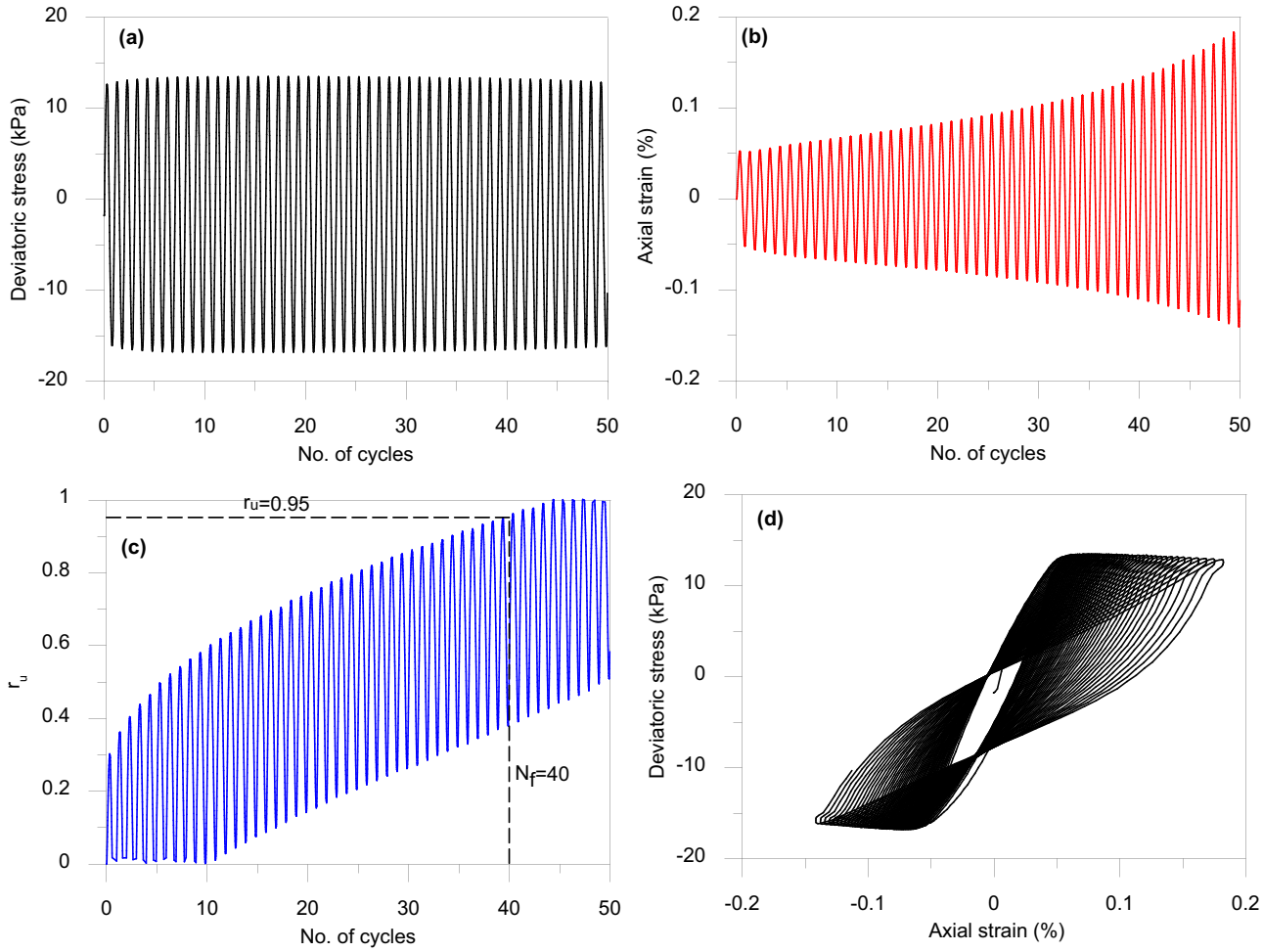

Fig. 5 Results of cyclic triaxial test of undisturbed samples BT-1'-T2-3, CSR = 0.305, and σ'_c = 24 kPa

typically observed. However, the liquefaction resistance of BT-1'-T1 (PI = 0 ~ 10%) is lower than that of BT-1'-T2 (non-plastic), which is opposite to the typical observation. This is because BT-1'-T2 has FC ~ 50% that is observed at the boundary of SM and ML (i.e., FC = 50%). In contrast, the FC of BT-1'-T1 is less than 50% at some locations. The test results indicate that low plastic clay (BT-1-T2) is also susceptible to soil liquefaction, which is consistent with the liquefaction susceptible criteria suggested by Seed et al. (2003) and Bray and Sancio (2006). This criterion states that fine-grain soils with PI < 12 are liquefiable and those with moderate plasticity (12 < PI < 18) can still undergo liquefaction when shaken intensely for a significant number of loading cycles. For soil liquefaction, a linear relationship between cyclic resistant ratio (CRR) and number of cycles N_f in log–log space is obtained from laboratory tests (Cetin and Bilge 2012; Idriss and Boulanger 2008b; Liu et al. 2001).

$$\mathrm{CRR} = \mathrm{a} \cdot N_f^{-b} \tag{2}$$

where a and b are two fitting parameters. The regression results of the above equation are shown in Fig. 6. The obtained values of b (slopes) of the three soils are close to that of clay (0.14) but lower than that of clean sand (0.34),

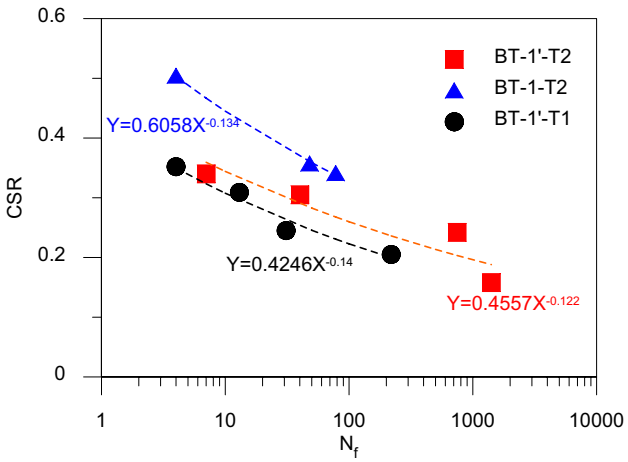

Fig. 6 Liquefaction resistance curve of undisturbed soil sample

as summarized in Idriss and Boulanger (2007). Therefore, the result of this study indicates that the high FC of the three soils can influence the value of *b* and exhibits similar trends as that of fine grain soil. Overall, a CSR corresponding to $N_f = 15$ ($CSR_{Nf=15}$) for SM and ML is relatively high (0.327 and 0.291, respectively), given the low blowcount (3 ~ 6) of the same layer (Fig. 3). This is because of the very high FC and low confining pressure applied on these samples, as discussed considering the test results of the remolded samples.

Liquefaction resistance from remolded sample

Influence of fines content

Figure 7 shows the comparison of the liquefaction resistances of different FCs under the conditions of γ_d~1.68 t/m^3 and $\sigma_c^{'}$ =24 kPa. As FC increases, liquefaction resistance increases. All curves of different FCs seem to be parallel to each other (i.e., the slopes are similar). However, the low FC leads to a slightly higher value of *b*, which is consistent with the trend reported in Boulanger and Idriss (2007) and Idriss and Boulanger (2006), as discussed earlier. Similar values of *b* indicate that the relative influence of large and small CSR amplitudes is similar for the soils with different FCs. Figure 8 shows that $CRR_{Nf=15}$ and FCs can be approximately associated through a linear relationship. As FCs increase, $CRR_{Nf=15}$ increases as well. During the empirical liquefaction potential analysis, blowcount requires further correction to estimate the liquefaction resistance of soil containing certain amounts of fines. The corrected (or equivalent) blowcount is typically higher than that measured for soil with certain FC (Idriss and Boulanger 2008a; Seed et al. 2003); (Tsai et al. 2019; Youd et al. 2001), resulting in a higher liquefaction resistance, which is consistent with the findings of this study.

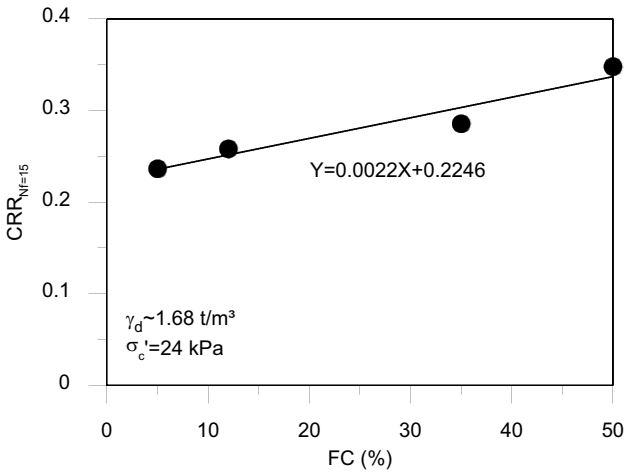

Fig. 8 Relationship between $CRR_{Nf=15}$ and FC

Influence of dry density

Figure 9 shows the liquefaction resistance at different dry densities with $\sigma_c^{'}$=24 kPa and FC = 5%. For some given values of γ_d, only one or two tests under different CSRs were performed and, thus, a liquefaction resistance curve could not be constructed. However, based on the previous observation and test results of various values of γ_d, the liquefaction resistance curves appear parallel for different values of γ_d. Therefore, given the assumption of the same slope for different values of γ_d, the liquefaction resistance curves for γ_d = 1.41, 1.61, 1.73 t/m^3 (presented by the dashed line Fig. 10) were constructed based on those for γ_d = 1.69 and 1.52 t/m^3. Figure 10 shows the relationship between $CRR_{Nf=15}$ and γ_d, which is expressed as a hyperbolic function as follows:

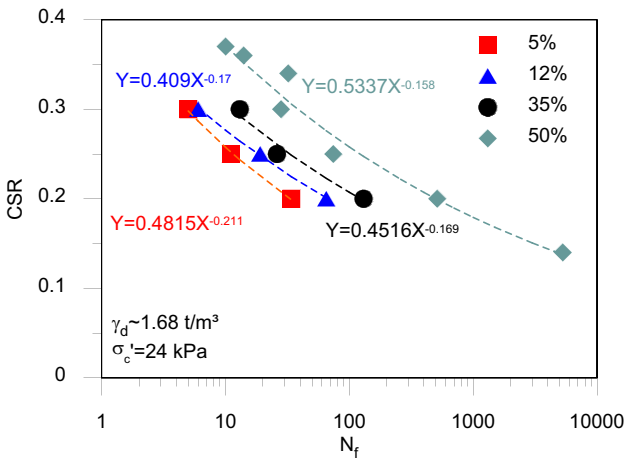

Fig. 7 Liquefaction resistance curve of remolded soil sample with different FCs

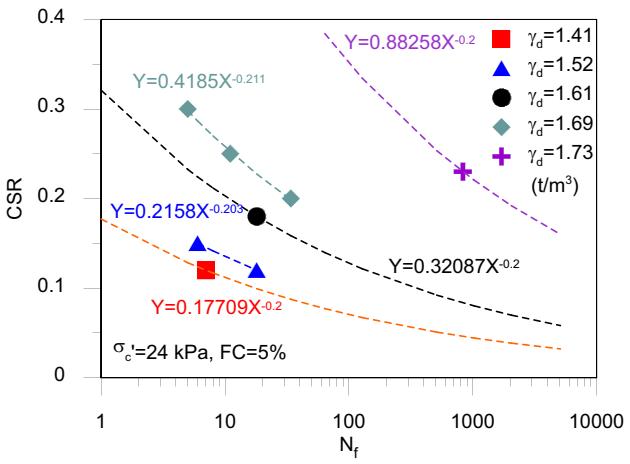

Fig. 9 Liquefaction resistance curve of remolded soil sample with different dry densities (t/m^3)

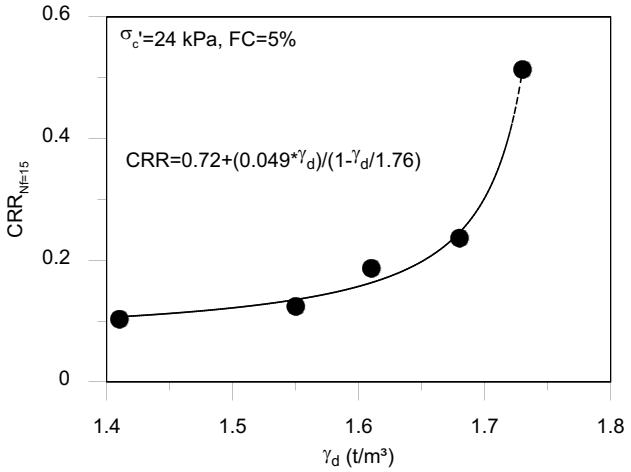

Fig. 10 Relationship between $CRR_{Nf=15}$ and dry densities

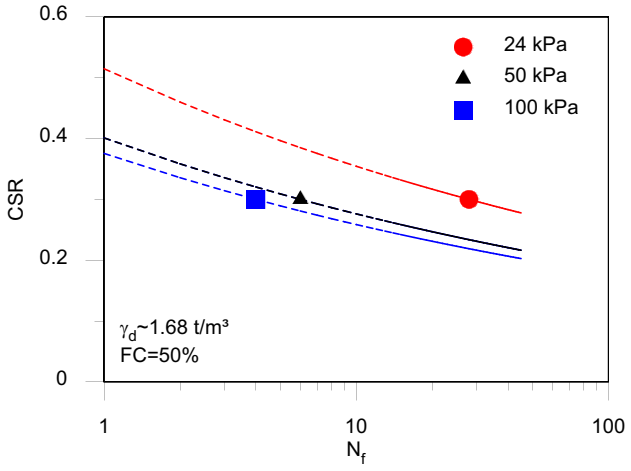

Fig. 11 Relationship between N_f and CSR at different confining pressures. The data points are of the test results, and the curve is constructed assuming $b = 0.158$

$$CRR = A + \frac{B\gamma_d}{1 - \gamma_d / C} \tag{3}$$

where A, B, and C are fitting parameters. This function form was adopted in Huang and Yang (2001) to construct an empirical liquefaction resistance curve as a function of N-values of the SPT. Parameter A represents the threshold (minimum) CSR to trigger liquefaction, and C represents the upper bound γ_d at which liquefaction does not occur. Similar to previous studies based on case histories and laboratory data, a higher value of γ_d leads to a higher liquefaction resistance. However, because $CRR_{Nf=15}$ of the highest dry density (1.73 t/m^3) is based on only one data point and interpreted given an assumption of same slope of resistance curve for different γ_d, the $CRR_{Nf=15}$ and γ_d curve at high dry density should be used with caution.

Influence of confining pressure

Figure 11 shows the liquefaction resistance at different confining pressures with FC = 50%, γ_d~1.68 t/m^3, and CSR = 0.3. A constant slope of $b = 0.158$ is assumed given that consolidation stress levels have a minor influence on b (Wichtmann 2016). As the confining pressure increases, the number of cycles required for liquefaction (i.e., liquefaction resistance) decreases even when the same CSR is applied. Although the applied CSR is the same, the actual cyclic deviatoric stress is higher due to higher confining pressure, as expressed in Eq. (1). Thus, N_f is less given the high confining pressure. This observation is consistent with the previous study (Harder and Boulanger 1997) and also confirms the requirement of the overburden correction in the empirical procedure to estimate liquefaction resistance (Seed 1983). According to Seed (1983), overburden correction is defined as follows:

$$K_\sigma = \frac{CRR_{\sigma_c'}}{CRR_{\sigma_{c=1}'}} \tag{4}$$

where $CRR_{\sigma_c'}$ is the CRR of a soil under a specific value of effective consolidation pressure σ_c' and $CRR_{\sigma_{c=1}'}$ is the CRR of the same soil when $\sigma_c' = 1$ atm (~100 kPa). To calculate K_σ, $CRR_{Nf=15}$ is calculated for different confining pressures assuming the same value of b (0.158). Then, the value of K_σ is obtained using Eq. (4) and compared with that determined in a previous study, as shown in Fig. 12. The obtained value of K_σ agrees well with that of the previous study (Harder and Boulanger 1997).

Discussion

Aging effect

The aging effect increases the liquefaction resistance in an old deposit, and, thus, soil liquefaction typically occurs in artificial lands or young alluvium deposits. The effect of diagenesis on liquefaction resistance based on laboratory cyclic triaxial or cyclic simple shear tests is quantified using the correction factor K_{DR}, which is expressed as follows (Seed 1979):

$$K_{DR} = \frac{CRR_{\text{undisturbed}}}{CRR_{\text{remolded}}} \tag{5}$$

where $CRR_{\text{undisturbed}}$ is the CRR of a high-quality undisturbed laboratory specimen, and CRR_{remolded} is the CRR of a freshly remolded laboratory specimen prepared at the same density and macrostructure using the same material. $CRR_{\text{undisturbed}}$

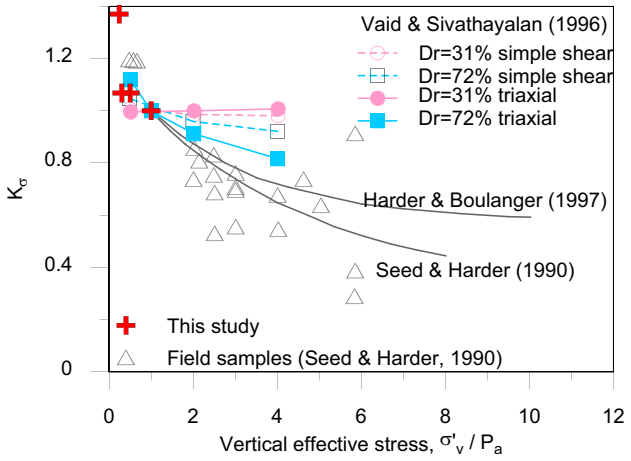

Fig. 12 Comparison of K_σ obtained in this study and previous study

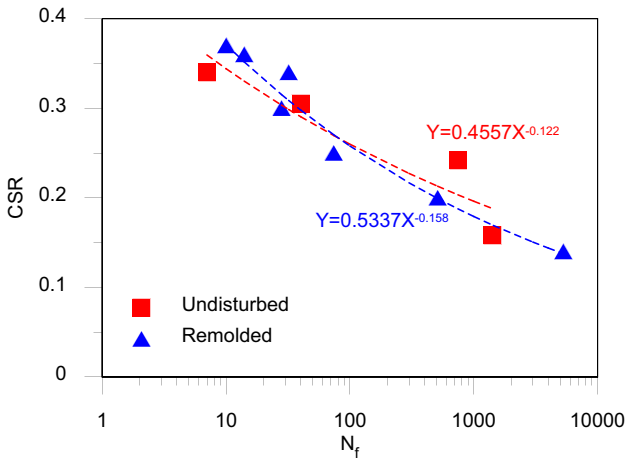

Fig. 13 Comparison of liquefaction resistance curve of remolded and undisturbed samples

is typically greater than CRR_{remolded}, as observed in the previous studies (Arango and Migues 1996; Bwambale et al. 2017; Chen and You 2004; Hayati and Andrus 2009; Ishihara 1985; Kiyota et al. 2009; Kokusho et al. 2012; Ladd 1982; Moss et al. 2008; Seed 1979; Tatsuoka et al. 1988; Taylor 2015; Troncoso et al. 1988). Therefore, the test results of the undisturbed and remodeled samples under the same condition (i.e., FC ~ 50%, γ_d ~ 1.68 t/m^3, and $\sigma_c^{'}$ =24 kPa) are compared and discussed, as shown in Fig. 13, to investigate the aging effect. Interestingly, the liquefaction resistances of the undisturbed and remodeled samples are similar. This result is different from expected trends observed in previous studies. The reason for the minor difference between the undisturbed and remodeled samples could be:

1. Undisturbed soil was disturbed during the sampling process, and, thus, the aging effect is demolished.
2. Undisturbed soil is retrieved from the site subjected to recurring liquefaction. The recent liquefaction phenomenon could lead to large strains in soil, which may eliminate the aging effect.

In this study, the undisturbed sample was retrieved using the gel-push sampling method (Lee et al. 2012; Taylor et al. 2012; Umehara et al. 2015) that has been proved to obtain high-quality undisturbed samples (Taylor et al. 2012). Therefore, the influence of sample disturbance is considered to be minor. As for the second argument, the hypothesis has been supported by the laboratory tests. Okamura et al. (2019) found that repeated small shaking events due to earthquakes significantly improve the liquefaction resistance of soils. However, the occurrence of extensive liquefaction alleviated the positive effects that were acquired through the series of pre-shaking events, and the liquefaction resistance of the sand was restored to a value equal to or even less than the initial value. This was quite similar to the observations in El-Sekelly et al. (2016a); El-Sekelly et al. (2016b); and Goto and Towhata (2014), confirming the conclusion reached in Dobry and Abdoun (2015) that the aging effect is reset due to liquefaction that induces large strains and eliminates the aging effect. This mechanism also explains why once a site is liquefied, it is highly vulnerable to soil liquefaction in the next event.

Comparison of in situ and laboratory soil liquefaction resistance curves

The liquefaction resistance from the laboratory test results is constructed by the procedure illustrated in Fig. 14, considering the state of stress and the multi-directional shearing effects. The detail to construct experimental liquefaction resistance curve and its comparison with the empirical one is described in the following. Figure 15a shows the comparison of the liquefaction resistance curve obtained in this study and the empirical curve based on the in situ data (Huang and Yang 2001). The curve obtained in this study (the red curve of Fig. 14c) is modified from the curve in Fig. 10 by correcting to $\sigma_c^{'}$ = 1 atm and using K_σ = 1.2, as per Eq. (4) and Fig. 12. In addition, the factor that converts 1D shearing in the laboratory to 2D shearing in the field is 0.8 according to Ueng and Lee (2015). Afterwards, dry unit weights of 1.5 and 1.9 t/m^3 are aligned with blowcount of 5 and 40, respectively, according to Anbazhagan et al. (2016), where $(N_{1,60})_{cs}$ represents the blowcount corrected to $\sigma_c^{'}$ = 1 atm and energy ratio = 60% for clean sand. On the other hand, the empirical curve is derived from the analysis of the liquefaction/non-liquefaction case during the 1999 Chi-Chi earthquake, Taiwan, as shown in Fig. 15a. It can be observed from Fig. 15a that the threshold CRR obtained from both studies is similar,

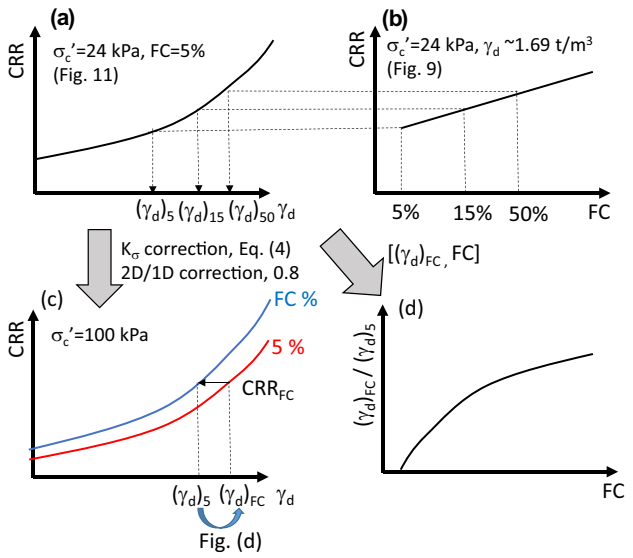

Fig. 14 Illustration of procedure to construct the laboratory soil resistance curve

which is approximate 0.1. However, the curve obtained in this study is lower than the in situ empirical curve when $N_{1,60} < 25$ and higher when $N_{1,60} > 25$. Nevertheless, both curves distinguish the liquefaction and non-liquefaction cases well in the high-blowcount range because rare data is available to define the boundary in this range. Although the discrepancy is observed, the curve of this study well defines the lower bound of the field liquefaction case at the study site (red points in Fig. 15a). The field data of the study site, constructed on basis of the boring information (Fig. 3) and the ground shaking information (Table 1), is also lower than that collected during the 1999 Chi-Chi earthquake. A possible reason for the inconsistency in the low-blowcount range is the aging effect, which has been discussed earlier. In this study, the liquefaction resistance curve is based on remolded or an undisturbed samples obtained from a site subjected to recurring liquefaction, which may eliminate the aging effect, whereas the empirical curve is based on the field data that include the aging effect. Therefore, the difference in CRR for the given same density may be attributed to the aging effect, as reported in Okamura et al. (2019), where the liquefaction resistance curve of an artificial land (Dobry et al. 2015) is lower than that of an old deposit (Andrus and Stokoe 2000). In other words, the liquefaction resistance curve of the site subjected to recurring liquefaction could be lower than the typical empirical curve that aggregates all sites, including the aging effect.

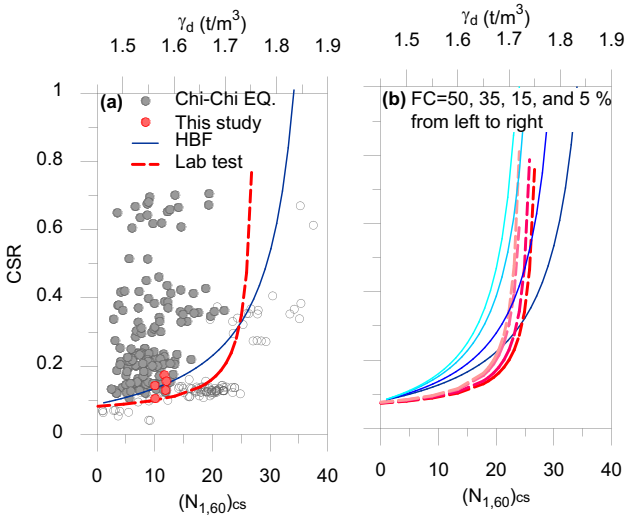

Fig. 15 **a** Comparison of in situ (Huwang and Yang 2001), lab (this study) soil resistance curve, and liquefaction (solid symbol)/non-liquefaction (solid symbol) data during the 1999 Chi-Chi earthquake and this study. **b** Comparison of in situ (blue thin curve) and lab (red bold curve) soil resistance at different FCs.

Figure 15b shows the comparison of the liquefaction resistance curve obtained in this study and the empirical curve for different FCs. As illustrated in Fig. 14, the liquefaction resistance curves for FCs other than 5% are established using the equivalent density of the associated FC, which is similar to the concept of the equivalent blowcount that accounts for the FC effect. As shown in Fig. 14a, b, the equivalent density is estimated by determining the density (per Fig. 10) for the given CRR of the associated FC (per Fig. 8). Next, the correlation between equivalent density and FC is established in Fig. 14d. In the last step, the equivalent density obtained from Fig. 14d given FC is used to estimate equivalent soil resistance as shown in Fig. 14c. Similarly, the empirical resistance curve for different FCs is constructed using the equivalent blowcount suggested by Huang and Yang (2001). It is observed that the FC effect in this study is not as significant as that in the in situ empirical curve, as indicated by the narrow distribution of curves at different FCs in this study. The difference could be attributed to different characteristic of fines (Bray and Sancio 2006; Seed et al. 2003). The fines used in this study are non-plastic, which may not have a significant impact on liquefaction resistance compared to the plastic fines.

Conclusion

This study conducts a series of experimental tests on the undisturbed and remolded samples obtained from a site in Taiwan subjected to recurring liquefaction. Undrained dynamic cyclic tests were performed on the undisturbed sample to assess the soil liquefaction resistance of the site. Different FCs, dry densities, and effective confining pressures were considered to remold the specimen during the test

program to investigate their influence on the soil liquefaction resistance. The liquefaction resistance associated with the aging effect due to the recurring liquefaction was discussed and compared with the other field and laboratory observation. Based on the experimental results and the insightful discussion, the following conclusions were accomplished:

1. The undisturbed BT-1'-T2 sample is non-uniform graded (Cu = 1.2) with non-plastic fines up to ~ 50% while the undisturbed BT-1'-T1 and BT-1-T2 sample has 25 ~ 60% low plastic fines (PI = 0–10% and 10–19%, respectively). All these samples are susceptible to soil liquefaction in terms of FC and plasticity (Bray and Sancio 2006; Seed et al. 2003), confirmed by the cyclic trixial test in this study.
2. Under the same soil condition of the remolded samples and the undisturbed samples, different FCs do not significantly affect the decay trend of the soil liquefaction resistance curve (i.e., the slope *b* is similar); however, the amount of FCs causes a shift in the soil liquefaction resistance curve. The relationship between $CRR_{Nf=15}$ and FC is positively correlated when the FC is below 50%. However, the FC effect (or correction) observed in this study is not as significant as that suggested by the in situ empirical curve by Huang and Yang (2001) that is also based on the Taiwan local data. The difference is because only non-plastic fines are considered in the remolded specimen in the test program.
3. Under the same FC and CSR conditions, the number of loading cycles, when the liquefaction occurs, decreases with higher effective confining stress. The obtained pressure correction factor K_σ agrees with the previous study (Harder and Boulanger 1997).
4. The soil liquefaction resistance curves of the remolded and undisturbed samples are similar, and their $CRR_{Nf=15}$ is not very different either. This may be because the recent liquefaction of the site resets the aging effect due to large induced strains and causes the undisturbed samples to behave like the remolded one in terms of the liquefaction resistance. The hypothesis has been supported by the field observation (Heidari and Andrus 2012) and the centrifuge tests on the specimen subjected to a series of shaking (El-Sekelly et al. 2016a, b; Okamura et al. 2019). However, it requires further verification by the direct comparison between soil testing before and after soil liquefaction.
5. CRR increases as the dry density of soil increases. Therefore, an experimental soil liquefaction curve (CRR vs γ_d) is constructed based on the hyperbolic model and converted to CRR vs $(N_{1,60})_{cs}$. Compared to the in situ empirical curve by Huang and Yang (2001) for Taiwan, the threshold CRRs to cause liquefaction are similar (~ 0.1); however, the rest of curve obtained in this study is lower. As reported in Okamura et al. (2019), this may be because the liquefaction resistance curve in this study is based on a remolded or an undisturbed sample obtained from a site subjected to recurring liquefaction, thereby eliminating the aging effect, whereas the empirical curve is based on field data that shall include the aging effect.
6. Based on 4 and 5, the liquefaction resistance curve of the site subjected to recurring liquefaction is lower than the typical empirical curve that aggregates all sites and includes the aging effect. In other words, a liquefaction site that has been subjected to recurring liquefaction is more vulnerable to liquefaction in a future event.

Funding This research was funded by the Central Geological Survey (CGS) in the framework of the "probabilistic liquefaction hazard analysis and its application" project. The financial support by the CGS is gratefully acknowledged. The tests have been performed with the help of W.C. Lin, who is a research assistant at the NCHU soil mechanics laboratory and graduate students of NTU, Y.H Yang, and Y.H. Lin.

References

Amini PF, Huang D, Wang G, Jin F (2021) Effects of strain history and induced anisotropy on reliquefaction resistance of toyoura sand. J Geotech Geoenviron Eng 147. https://doi.org/10.1061/(ASCE)GT.1943-5606.0002588

Anbazhagan P, Uday A, Moustafa SSR, Al-Arif NSN (2016) Correlation of densities with shear wave velocities and SPT N values. J Geophys Eng 13:320–341

Andrus RD, Stokoe KH (2000) Liquefaction resistance of soils from shear-wave velocity. J Geotech Geoenviron Eng 126:1015–1025

Arango I, Migues RE (1996) Investigation of the seismic liquefaction of old sand deposits. Bechtel Corporation, San Francisco, CA

Boulanger RW, Idriss IM (2007) Evaluation of cyclic softening in silts and clays. J Geotech Geoenviron Eng, ASCE 133:641–652

Bray JD, Sancio RB (2006) Assessment of the liquefaction susceptibility of fine-grained soils. J Geotech Geoenviron Eng 132:1165–1177

Bwambale B, Andrus RD, Cubrinovski M (2017) Influence of age on liquefaction resistance of Holocene alluvial and marine soils in Christchurch and Kaiapoi, New Zealand. In: proceedings of the 3rd international conference on performance-based design in earthquake geotechnical engineering (PBD-III), Vancouver, Canada

Cetin KO, Bilge HT (2012) Cyclic large strain and induced pore pressure models for saturated clean sands. J Geotech Geoenviron Eng 138:309–323

Chen Y, You P (2004) Evaluation of liquefaction potential by the test results of in-situ frozen samples. In: Matsui TCJ, Michel JL, Allersma H (ed) International society of offshore and polar engineers (ISOPE). Cupertino, California 2004: proceedings of the 14th international offshore and polar engineering conference, Toulon, France, pp 563–570

Dobry R, Abdoun T (2015) Cyclic shear strain needed for liquefaction triggering and assessment of overburden pressure factor Kσ. J Geotech Geoenviron Eng, ASCE 141:04015047–04015041 to -04015018

Dobry R, Abdoun T, Stokoe IKH, Moss RES, Hatton M, El Ganainy H (2015) Liquefaction potential of recent fills versus natural sands located in high-seismicity regions using shear-wave velocity.

Geotech Geoenviron Eng ASCE 141:04014112. https://doi.org/10.1061/(ASCE)GT.1943-5606.0001239
Darby KM, Boulanger RW, DeJong JT, Bronner JD (2019) Progressive changes in liquefaction and cone penetration resistance across multiple shaking events in centrifuge tests. J Geotech Geoenviron Eng 145:04018112. https://doi.org/10.1061/(ASCE)GT.1943-5606.0001995
El-Sekelly W, Abdoun T, Dobry R (2016a) Liquefaction resistance of a silty sand deposit subjected to preshaking followed by extensive liquefaction. J Geotech Geoenviron Eng, ASCE 142:04015101. https://doi.org/10.1061/(ASCE)GT.1943-5606.000144404015101
El-Sekelly W, Dobry R, Abdoun T, Steidl JH (2016b) Centrifuge modeling of the effect of preshaking on the liquefaction resistance of silty sand deposits. J Geotech Geoenviron Eng, ASCE 142:04016012. https://doi.org/10.1061/(ASCE)GT.1943-5606.000143004016012
Goto S, Towhata I (2014) Acceleration of aging effect of drained cyclic pre – shearing and high temperature consolidation on liquefaction resistance of sandy soils. Geotechnical Eng J, JGS 9:707–719
Harder LF, Boulanger RW (1997) Application of Kσ and Kα correction factors. In: proceedings, NCEER workshop on evaluation of liquefaction resistance of soils
Hayati H, Andrus RD (2009) Updated liquefaction resistance correction factors for aged sands. J Geotech Geoenviron Eng ASCE 135:1683–1692
Heidari T, Andrus RD (2012) Liquefaction potential assessment of pleistocene beach sands near Charleston, South Carolina. J Geotech Geoenviron Eng 138:1196–1208
Huang JH, Yang CW (2001) Verification of critical cyclic strength curve by Taiwan Chi-Chi earthquake data. Soil Dyn Earthq Eng 21:237–257
Idriss IM, Boulanger RW (2006) Semi-empirical procedures for evaluating liquefaction potential during earthquakes. Soil Dyn Earthq Eng 26:115–130
Idriss IM, Boulanger RW (2007) SPT- and CPT-based relationships for the residual shear strength of liquefied soils. In: KD Pitilakis (ed) Proc., 4th int. conf. on earthquake geotechnical engineering. Springer, New York, pp 1–22
Idriss IM, Boulanger RW (2008a) Soil liquefaction during earthquakes. EERI monograph. EERI
Idriss IM, Boulanger RW (2008b) Soil liquefaction during earthquakes. Paper presented at the Monograph MNO-12, earthquake engineering research institute, Berkeley, CA
Ishihara K (1985) Stability of natural deposits during earthquakes. In: AA B (ed) 11th international conference on soil mechanics and foundation engineering. Rotterdam, pp 321–376
Ishihara K (1993) Liquefaction and flow failure during earthquakes. Geotechnique 43:351
Kiyota T, Koseki J, Sato T, Kuwano R (2009) Aging effects on small strain shear moduli and liquefaction properties of in-situ frozen and reconstituted sandy soils. Soils Found 49:259–274
Kokusho T (2016) Major advances in liquefaction research by laboratory tests compared with insitu behavior. Soil Dyn Earthq Eng 91:3–22
Kokusho T, Nagao Y, Ito F, Fukuyama T (2012) Aging effect on sand liquefaction observed during the 2011 earthquake and basic laboratory studies. In: proceedings of the international symposium on engineering lessons learned from the 2011 great Japan earthquake. Tokyo, Japan, pp 759–770
Kondo Y (2013) Effects of sand ageing on liquefaction resistance in young reclaimed land in Urayasu City, University of Tokyo, Tokyo, Japan. (in Japanese)
Ladd R (1982) Geotechnical laboratory testing program for study and evaluation of liquefaction ground failure using stress and strain approaches: heber road site, October 15, 1979 imperial valley earthquake geological survey. vol I Wayne (NJ): woodward-clyde consultants. Award no: 14–08–001–19788 sponsored by the US geological survey
Lee WF, Ishihara K, Chen CC (2012) Liquefaction of silty sand – preliminary studies from recent Taiwan, New Zealand, and Japan earthquakes. In: proceedings of the international symposium on engineering lessons learned from the 2011 great east Japan earthquake. Tokyo, Japan
Liu AH, Stewart JP, Abrahamson NA, Moriwaki Y (2001) Equivalent number of uniform stress cycles for soil liquefaction analysis. J Geotech Geoenviron Eng 127:1017–1026
Mitchell JK, Solymer ZV (1984) Time-dependent strength gain in freshly deposited or densified sand. J Geotech Engng, ASCE 110:1559–1576
Moss RES, Thornhill DM, Nelson AI, Levulett DA (2008) Influence of aging on liquefaction potential: preliminary results. Geotech Earthq Eng Soil Dyn IV Congr ASCE:1–10. GSP 181
Okamura M, Nelson F, Watanabe S (2019) Pre-shaking effects on volumetric strain and cyclic strength of sand and comparison to unsaturated soils. Soil Dyn Earthq Eng 124:307–316
Price AB, DeJong JT, Boulanger RW (2017) Cyclic loading response of silt with multiple loading events. J Geotech Geoenviron Eng 143:04017080. https://doi.org/10.1061/(ASCE)GT.1943-5606.0001759
Quigley MC, Bastin S, Bradley BA (2013) Recurrent liquefaction in Christchurch, New Zealand, during the Canterbury earthquake sequence. Geology 41:419–422. https://doi.org/10.1130/G33944
Seed HB (1979) Soil liquefaction and cyclic mobility evaluation for level ground during earthquakes. J Geotech Eng Div ASCE 105:201–255
Seed HB (1983) Earthquake-resistant design of earth dams. In: proc., symp. seismic des. of earth dams and caverns, ASCE, New York, pp 41–64
Seed RB et al (2003) Recent advances in soil liquefaction engineering: a unified and consistent framework. Paper presented at the 26th annual geotechnical spring seminar, Los Angeles section of the geoInstitute, American society of civil engineers, Queen Mary, Long Beach, CA
Tatsuoka F, Kato H, Kimura M, Pradhan TBS (1988) Liquefaction strength of sands subjected to sustained pressure. Soils and Foundations 28 (1):119–131
Teparaksa J, Koseki J (2018) Effect of past history on liquefaction resistance of level ground in shaking table test. Géotech Lett 8:256–261. https://doi.org/10.1680/jgele.18.00085
Taylor M (2015) The geotechnical characterization of Christchurch sands for advanced soil modeling [dissertation]. University of Canterbury, Christchurch, New Zealand
Taylor ML, Cubrinovski M, Haycock I (2012) Application of new 'gel-push' sampling procedure to obtained high quality laboratory test data for advanced geotechnical analyses. In: proc. 12th New Zealand soc. of earthquake eng. conf., Christchurch, New Zealand
Towhata I, Taguchi Y, Hayashida T, Goto S, Shintaku Y, Hamada Y, Aoyama S (2017) Liquefaction perspective of soil ageing. Geotechnique 2017(67):467–478
Troncoso J, Ishihara K, Verdugo R (1988) Aging effects on cyclic shear strength of tailings materials. In: proceedings of the 9th world conference on earthquake engineering, vol. III. Japan: Tokyo-Kyoto, pp 121–126
Tsai C-C, Hwang Y-W, Lu C-C (2020) Liquefaction, building settlement, and residual strength of two residential areas during the 2016 southern Taiwan earthquake. Acta Geotechnica 15:1363–1379
Tsai C-C, Kishida T, Kuo C-H (2019) Unified correlation between SPT–N and shear wave velocity for a wide range of soil types considering strain-dependent behavior. Soil Dyn Earthq Eng 126

Tsai CC, Hsu SY, Wang KL, Yang HC, Chang WK, Chen CH, Hwang YW (2017) Geotechnical reconnaissance of the 2016 ML6.6 Meinong earthquake in Taiwan. J Earthq Eng

Ueng T-S, Lee C-A (2015) Pore pressure generation in saturated sand induced by one- and two-dimensional shakings. J Geo Eng 10(2):53, 10:53–61

Umehara Y, Chiaro G, Kiyota T, Hosona Y, Yagiura Y, Chiba H (2015) Effectiveness of 'gel-push' sampling technique to retrieve undisturbed sandy specimens for liquefaction test. In: 6th international conference on earthquake geotechnical engineering, Christchurch, New Zealand

Wahyudi S, Koseki J, Sato T, Chiaro G (2016) Multiple-liquefaction behavior of sand in cyclic simple stacked-ring shear tests. Int J Geomech 16:C4015001. https://doi.org/10.1061/(ASCE)GM.1943-5622.0000596

Wakamatsu K (2012) Recurrence of liquefaction at the same site induced by the 2011 great east Japan earthquake compared with previous earthquakes. Paper presented at the paper presented at the 15th world conference on earthquake engineering Lisbon Portugal

Wichtmann T (2016) Soil behaviour under cyclic loading - experimental observations, constitutive description and applications. Karlsruhe Insitude of Technology

Wichtmann T, Niemunis A, Triantafyllidis T, Poblete M (2005) Correlation of cyclic preloading with the liquefaction resistance. Soil Dyn Earthq Eng 25:923–932

Ye B, Hu H, Bao X, Lu P (2018) Reliquefaction behavior of sand and its mesoscopic mechanism. Soil Dyn Earthquake Eng 114:12–21. https://doi.org/10.1016/j.soildyn.2018.06.024

Youd TL (1984) Recurrence of liquefaction at the same site. In: proceedings of the 8th world conference on earthquake engineering. San Francisco, CA. Englewood Cliffs, NJ: Prentice-Hall, Inc, pp 231–238

Youd TL, Hoose SN (1977) Liquefaction susceptibility and geologic setting. In: proc., 6th world conf. on earthquake engrg. Prentice-Hall, Englewood Cliffs, N.J., pp 2189–2194

Youd TL et al (2001) Liquefaction resistance of soils: summary report from the 1996 NCEER and 1998 NCEER/NSF Workshops on evaluation of liquefaction resistance of soils. J Geotech Geoenviron Eng 127:817–833

Youd TL, Perkins DM (1978) Mapping of liquefactioninduced ground failure potential. J Geotech Engrg Div, ASCE 104:433–446